

Experimental and theoretical study for corrosion inhibition of mild steel 1 M HCl solution by some new diaminopropanenitrile compounds

L. Herrag · M. Bouklah · N. S. Patel · B. M. Mistry ·
B. Hammouti · S. Elkadiri · M. Bouachrine

Received: 23 September 2011 / Accepted: 11 January 2012 / Published online: 4 February 2012
© Springer Science+Business Media B.V. 2012

Abstract The inhibition of the corrosion of mild steel 1 M HCl solution by some diamine compounds has been investigated in relation to the concentration of the inhibitor as well as the temperature using weight loss and electrochemical measurements. The effect of the temperature on the corrosion behavior with the addition of different concentrations of new diamine compounds (3-[2-(2-cyano-ethylamino)-methylamino]-propionitrile (**P1**); 3-[2-(2-cyano-ethylamino)-ethylamino]-propionitrile (**P2**), and 3-[6-(2-cyano-ethylamino)-hexylamino]-propionitrile (**P3**), respectively, was studied in the temperature range 40–80 °C. Polarization curves reveal that (**P1**, **P2**, and **P3**) are mixed type inhibitors. The inhibition efficiency of organic compounds is temperature independent, but increases with the inhibitor concentration. Adsorption of inhibitor on the carbon steel surface is found to obey the Langmuir adsorption isotherm. Some thermodynamic functions of dissolution and adsorption processes were also determined. On the other hand, and in order to determine the relationship between the molecular structure of these compounds and inhibition efficiency, quantum chemical parameters were calculated. The theoretically obtained results were found to be consistent with the experimental data.

Keywords Diamine · Steel · Hydrochloric acid · Corrosion inhibitors

L. Herrag · M. Bouklah · B. Hammouti · S. Elkadiri
LCAE-URAC18, Faculté des Sciences, Université Mohammed Premier, 60000 Oujda, Morocco

N. S. Patel (✉) · B. M. Mistry
Applied Chemistry Department, S V National Institute of Technology, Surat 395007, Gujarat, India
e-mail: nikanetan.ptl@gmail.com

M. Bouachrine
UMIM, Faculté Polydisciplinaire de Taza, Université Sidi Mohamed Ben Abdellah, Taza, Morocco

Introduction

Carbon steel is widely used in industry. However, in industrial environments, the metal is subject to acid corrosion. The study of the corrosion of iron is a matter of tremendous theoretical and practical concern, and as such has received a considerable amount of interest [1]. Hydrochloric acid (HCl) solutions are widely used for pickling, cleaning, descaling, etc. of iron and steel. Corrosion inhibitors are needed to reduce the corrosion rates of metallic materials in this acid medium. One solution to this problem is the application of a corrosion inhibitor, compounds containing nitrogen, oxygen, and sulfur atoms generally give rise to satisfying inhibitor efficiency in the case of iron corrosion in HCl medium [2–5]. However, a great number of organic compounds have been used in this regard. The influence of nitrogenated organic compounds, such as amine and heterocyclic compounds, on the corrosion of steel has been well documented [6–16].

Diamine compounds have recently emerged as a new and potential class of corrosion inhibitors. A survey of the literature reveals that, despite the high ability of diamine compounds to interact strongly with the metal surface, little attention has been paid on the use of these compounds as corrosion inhibitors. In continuation of our work on the development of diamines as corrosion inhibitors in acidic media, we report here the inhibitory behavior of new diamine compounds 3-((2-[(2-cyanoethyl)amino]ethyl)amino)-propanenitrile (**P1**), 3-((3-[(2-cyanoethyl)amino]propyl)amino)-propanenitrile (**P2**), and 3-((6-[(2-cyanoethyl)amino]hexyl)amino)-propanenitrile (**P3**), respectively, on corrosion inhibition of mild steel (MS) in 1 M HCl solutions.

On the other hand, several quantum chemical methods and quantum-chemistry calculations have been performed to study the molecular structure and the reaction mechanisms in order to interpret the experimental results as well as to solve chemical ambiguities and to correlate the inhibition efficiency to the molecular properties [17, 18]. The structure and electronic parameters can be obtained by means of theoretical calculations using the computational methodologies of quantum chemistry. The geometry of the inhibitor in its ground state, as well as the nature of their molecular orbitals, highest occupied molecular orbital (HOMO) and lowest unoccupied molecular orbital (LUMO), are involved in the properties of activity of the inhibitors. The relationships between the structural parameters and corrosion inhibition of those compounds have not yet been studied.

The more relevant molecular properties on its action as inhibition of the corrosion of these three compounds were calculated. These properties are the HOMO energy (E_{HOMO}), the LUMO (E_{LUMO}), energy gap (ΔE), dipole moment (μ), electronegativity (χ), electron affinity (A), global hardness (η), softness (σ), ionization potential (I), the fraction of electrons transferred (ΔN), and the total energy (TE).

The aim of this work is devoted to study the inhibition characteristics of these compounds for acid corrosion of MS using weight loss and electrochemical measurements. Thermodynamic parameters such as adsorption heat, adsorption entropy, and adsorption-free energy can be obtained from experimental data of the studies of the inhibition process at different temperatures. The kinetic data, such as apparent activation energy and pre-exponential factor at different inhibitor

concentrations, are calculated, and the effects of the activation energy and pre-exponential factor on the corrosion rate of steel discussed.

Experimental details

Synthesis of diaminopropanenitrile compounds

The diamine derivatives, namely 3-[2-(2-cyano-ethylamino)-methylamino]-propionitrile (**P1**), 3-[2-(2-cyano-ethylamino)-ethylamino]-propionitrile (**P2**), and 3-[6-(2-cyano-ethylamino)-hexylamino]-propionitrile (**P3**), respectively, were synthesized as follows (Fig. 1).

Synthesis of 3-[2-(2-cyano-ethylamino)-methylamino]-propionitrile (**P1**)

Diaminomethylene solution (83.3 mmol, 5 g) cold at 0 °C and (166.6 mmol, 8.83 g) of acrylonitrile cold were stirred for 24 h in the dark to obtained the yellow oil with yield 96%.

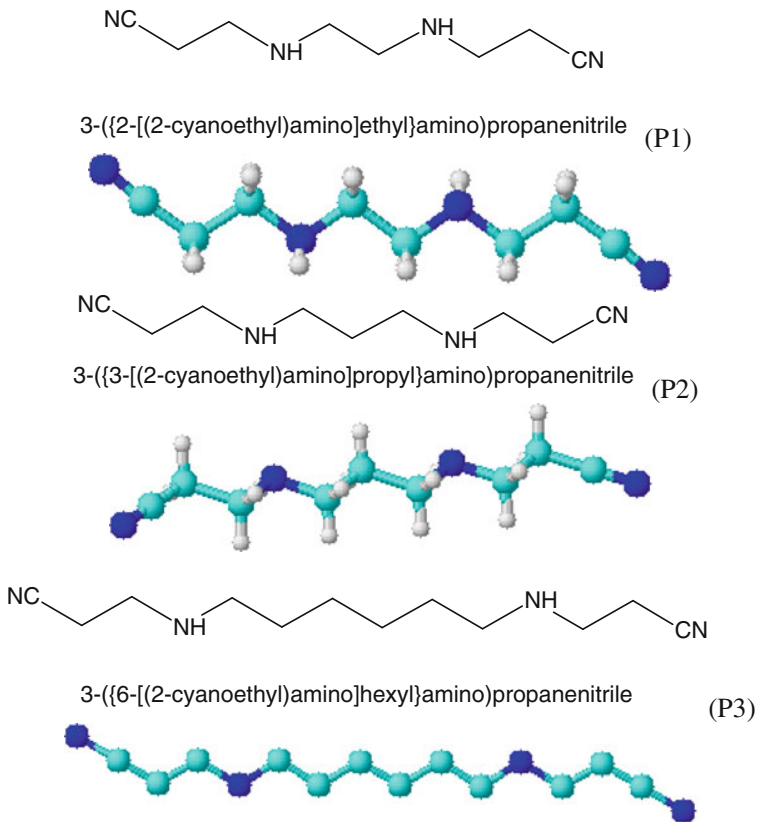


Fig. 1 Molecular formulae of the diamine compounds studied

$^1\text{H NMR}$ (300 MHz, CDCl_3): δ 2.83–2.87 (t, $J = 7.66$ Hz, 4H, $\text{CH}_2\text{--CH}_2\text{--CN}$), 2.67 (s, 4H, $\text{CH}_2\text{--NH}$), 2.43–2.47 (t, $J = 7.33$, 4H, $\text{CH}_2\text{--CH}_2\text{--CN}$), 1.39 (s, 2H, --NH). $^{13}\text{C NMR}$ (75 MHz, CDCl_3): δ 119.32 (C-9, C-11, $\text{--CH}_2\text{--CN}$), 48.68 (C-2, C-7, $\text{--CH}_2\text{--NH}$), 45.277 (C-4, C-5, $\text{--NH--CH}_2\text{--CH}_2\text{--NH--}$), 19.148 (C-1, C-8, $\text{--CH}_2\text{--CN}$), *EI-MS* (70 eV, *m/z*): 91 (0.5), 79 (0.1), 67 (0.5), 54 (59.8), 52 (3.2), 40 (2.7).

Synthesis of 3-[2-(2-cyano-ethylamino)-ethylamino]-propionitrile (**P2**)

Diaminoethylene solution (67.5 mmol, 5 g) cold at 0 °C and (135 mmol, 7.16 g) of acrylonitrile cold were stirred for 24 h in the dark to obtain the yellow oil with yield 95%.

$^1\text{H NMR}$ (300 MHz, CDCl_3): δ 2.83–2.87 (t, $J = 4$ Hz, 4H, $\text{CH}_2\text{--CH}_2\text{--CN}$), 2.65–2.78 (t, $J = 7.33$ Hz, 4H, $\text{CH}_2\text{--CH}_2\text{--NH}$), 2.44–2.50 (t, $J = 4$ Hz, 4H, $\text{CH}_2\text{--CH}_2\text{--CN}$), 1.65 (m, $J = 7.33$ Hz, 2H, $\text{CH}_2\text{--CH}_2\text{--NH}$), 1.15 (s, 2H, --NH). $^{13}\text{C NMR}$ (75 MHz, CDCl_3): δ 119.351 (C-10, C-12, $\text{--CH}_2\text{--CN}$), 48.167 (C-2, C-8, $\text{--CH}_2\text{--NH}$), 45.432 (C-4, C-6, $\text{--NH--CH}_2\text{--CH}_2\text{--NH--}$), 30.043 (C-5, $\text{--NH--CH}_2\text{--CH}_2\text{--CH}_2\text{--NH--}$), 19.018 (C-1, C-9, $\text{--CH}_2\text{--CN}$). *EI-MS* (70 eV, *m/z*): 91 (2.3), 52 (3.5), 40 (5.6).

Synthesis of 3-[6-(2-cyano-ethylamino)-hexylamino]-propionitrile (**P3**)

Diaminohexamethylene solution (8.6 mmol, 1 g) cold at 0 °C and (17.2 mmol, 0.91 g) of acrylonitrile cold were stirred for 24 h in the dark to obtain the yellow oil with yield 84%.

$^1\text{H NMR}$ (300 MHz, CDCl_3): δ 2.9–3 (t, $J = 7.8$ Hz, 4H, $\text{CH}_2\text{--CH}_2\text{--CN}$), 2.55–2.65 (t, $J = 7.7$ Hz, 4H, $\text{CH}_2\text{--CH}_2\text{--NH}$), 1.2–1.6 (m, 12H, $(\text{CH}_2)_6\text{--NH}$), 1.18 (s, 2H, --NH). $^{13}\text{C NMR}$ (75 MHz, CDCl_3): δ 119 (C-13, C-15, $\text{--CH}_2\text{--CN}$), 49 (C-4, C-9, $\text{--CH}_2\text{--NH}$), 45 (C-2, C-11, $\text{--NH--CH}_2\text{--CH}_2\text{--NH--}$), 30 (C-5, C-8, $\text{--NH--}(\text{CH}_2)_6$), 27 (C-2, C-11, $\text{--CH}_2\text{--CH}_2\text{--}$), 19 (C-1, C-12, $\text{--CH}_2\text{--CN}$).

Material preparation

Corrosion tests were carried out on electrodes cut from sheets of MS. Steel containing 0.09% P, 0.38% Si, 0.01% Al, 0.05% Mn, 0.21% C, 0.05% S, and the remainder iron were used for the measurement of weight loss and electrochemical studies. The surface preparation of the specimens was carried out using emery paper with different grit sizes ranging from 260 to 1,200; they were degreased with AR grade ethanol and acetone, and dried at room temperature before use. The solutions (1 M HCl) were prepared by dilution of an analytical reagent grade 37% HCl with double-distilled water. The solubility of the tested diamine compounds are about 10^{-3} M in 1 M HCl solution.

Methods

Gravimetric measurements

For weight loss measurements, each run was carried out in a double-walled glass cell equipped with a thermostat-cooling condenser containing 100 ml test solution.

The steel specimens used had a rectangular form ($1.5 \times 1.5 \times 0.05$ cm) and was completely immersed at inclined position in the vessel. The immersion time for the weight loss was 6 h at 35 °C. After 6 h of immersion, the electrode was withdrawn, rinsed with double-distilled water, washed with ethanol, dried, and weighed. Duplicate experiments were performed in each case and the mean value of the weight loss was reported. The weight loss was used to calculate the corrosion rate (W) in milligrams per square centimetre per hour ($\text{mg cm}^{-2} \text{h}^{-1}$).

Polarisation measurements

Electrochemical measurements were carried out in conventional three-electrode cylindrical Pyrex glass cells. The working electrode was a disc cut from MS with the composition described above. The area exposed to the corrosive solution was 1 cm^2 . A platinum electrode and saturated calomel electrode (SCE) were used, respectively, as auxiliary and reference electrodes. All potentials are given in the SCE scale. The cell was thermostated at 35 °C.

The polarization curves were recorded with a potentiostat type AMEL 550 using a linear sweep generator type AMEL 567 at a scan rate of 30 mV/min. Before recording the cathodic potentiokinetic curves up the corrosion potential, the MS electrode was polarized at -800 mV/SCE for 10 min.

However, for anodic polarization curves, the potential of the working electrode was swept from its open circuit potential value after 30 min at rest. Solutions were de-aerated with nitrogen. The nitrogen bubbling was maintained in the solutions during the electrode chemical measurements.

Computational details

Density functional theory (DFT) methods were used in this study. These methods have become very popular in recent years because they can reach exactitude similar to other methods in less time and are less expensive from the computational point of view. In agreement with the DFT results, energy of the fundamental state of a polyelectronic system can be expressed through the total electronic density, and, in fact, the use of electronic density instead of wave function for calculating the energy constitutes the fundamental base of DFT [19]. All calculations were done by GAUSSIAN 03 W software [20], using the B3LYP functional [21] and a 6-31G* basis set [22]. The B3LYP, a version of the DFT method, uses Becke's three-parameter functional (B3) and includes a mixture of HF with DFT exchange terms associated with the gradient-corrected correlation functional of Lee, Yang, and Parr (LYP). The geometry of all species under investigation was determined by optimizing all geometrical variables without any symmetry constraints. Frontier molecular orbitals (HOMO and LUMO) may be used to predict the adsorption centers of the inhibitor molecule. For the simplest transfer of electrons, adsorption should occur at the part of the molecule where the softness, σ , which is a local property, has the highest value. According to Koopman's theorem [23], the energies of the HOMO and the LUMO orbitals of the inhibitor molecule are related to the ionization potential, I , and the electron affinity, A , respectively, by the following

relationships: $I = -E_{HOMO}$ and $A = -E_{LUMO}$. Absolute electronegativity, χ , and absolute hardness, η , of the inhibitor molecule are given by [24]. $\chi = \frac{I+A}{2}$ and $\eta = \frac{I-A}{2}$. The softness is the inverse of the hardness: $\sigma = \frac{1}{\eta}$.

Results and discussion

Weight loss measurements

The corrosion of MS in 1 M HCl medium containing various concentrations of some diamine compounds was studied by weight loss measurements. In this case, the inhibition efficiency of inhibitor, E (%), is calculated by applying the following equation:

$$E\% = \frac{W_{\text{corr}} - W_{\text{corr(inh)}}}{W_{\text{corr}}} \times 100 \quad (1)$$

where W_{corr} and $W_{\text{corr(inh)}}$ are the corrosion rates of MS in the absence and presence of inhibitor molecule, respectively. Table 1 summarizes the corrosion rates (W) of MS and the E (%) for some diamine compounds studied at different concentrations. It is obvious from these data that all of these compounds inhibit the corrosion of MS in 1 M HCl solution at all concentrations used in this study, and that the corrosion rate was seen to decrease with increasing additive concentrations at 35 °C. We note that at a lower concentration (10^{-6} M), **P3** exhibits the best inhibitory effect near those of **P1** and **P2**, because **P3** is the longest molecule. At 10^{-3} M, E (%) attains 98% for **P2**. Thus, we assume that this inhibitor is the better inhibitor for the MS, and E (%) was found to be in the following order: **P2** > **P1** = **P3**. The difference in their inhibitive action can be explained based on the effect of chain length, as pointed by Touhami et al. [25] in their study on the effect on nature and length of carbonic chain joining two pyrazolic cycles. They showed that the inhibition efficiency of bipyrazolic compounds decreases with the carbonic chain length joining the pyrazolic cycles. As a result of this classification, and in order to better understand the inhibition mechanism of organic compounds studied, a detailed study using electrochemical polarization was carried out.

Potentiodynamic polarisation

Figure 2 shows the cathodic and anodic polarisation curves of MS in 1 M HCl blank solution and in the presence of different concentrations (10^{-3} – 10^{-6} M) of some diamine compounds studied. With the increase of organic compounds concentrations, both anodic and cathodic currents were inhibited. This result shows that the addition of inhibitor reduces anodic dissolution and also retards the hydrogen evolution reaction.

Table 2 gives the values of kinetic corrosion parameters as the corrosion potential E_{corr} , corrosion current density I_{corr} , Tafel slope b_c , and inhibition efficiency for the corrosion of MS in 1 M HCl solution with different concentrations of inhibitor.

Table 1 Corrosion parameters obtained from weight loss of MS in 1 M HCl containing various concentrations of some diamine compounds at 35 °C

Inhibitor	Concentration (M)	W (mg cm ⁻² h ⁻¹)	E (%)
Blank	1	1.44	–
P1	10 ⁻⁶	0.69	52.08
	10 ⁻⁵	0.29	79.86
	5 × 10 ⁻⁵	0.16	88.88
	10 ⁻⁴	0.13	90.97
	5 × 10 ⁻⁴	0.12	91.66
	10 ⁻³	0.09	93.75
P2	10 ⁻⁶	0.41	71.52
	10 ⁻⁵	0.19	86.80
	5 × 10 ⁻⁵	0.16	88.88
	10 ⁻⁴	0.12	91.66
	5 × 10 ⁻⁴	0.09	93.75
	10 ⁻³	0.03	97.91
P3	10 ⁻⁶	0.22	84.72
	10 ⁻⁵	0.2	86.11
	5 × 10 ⁻⁵	0.17	88.19
	10 ⁻⁴	0.16	88.88
	5 × 10 ⁻⁴	0.13	90.97
	10 ⁻³	0.09	93.75

The corrosion current densities were estimated by Tafel extrapolation of the cathodic curves to the open circuit corrosion potential.

From Table 2, it can be concluded that:

- The I_{corr} values decrease with increasing inhibitor concentration.
- Adsorption of organic inhibitor molecules onto a metal surface retards the metal dissolution, and as a consequence hydrogen evolution by blocking the active sites on the MS, or can even screen the covered part of the electrode and therefore protect it from the action of the corrosion medium. The addition of some compounds produces slight changes in the values of E_{corr} and b_c . The variation of b_c values with alteration in type and concentration of inhibitors indicated that there was an influence of the added compounds on the kinetics of hydrogen evolution. This indicates [26] that the adsorbed molecules of the inhibitor do not affect the mechanism of hydrogen evolution.
- The values of inhibition efficiency ($E_1\%$) increase with inhibitor concentration reaching a maximum value (88.2%) at 10⁻³ M.
- The diamine compounds have acted as mixed type inhibitors.

Effect of temperature

Temperature can affect the steel corrosion in the acidic media in the presence and absence of inhibitors. Generally, the corrosion rate increases with the rise of

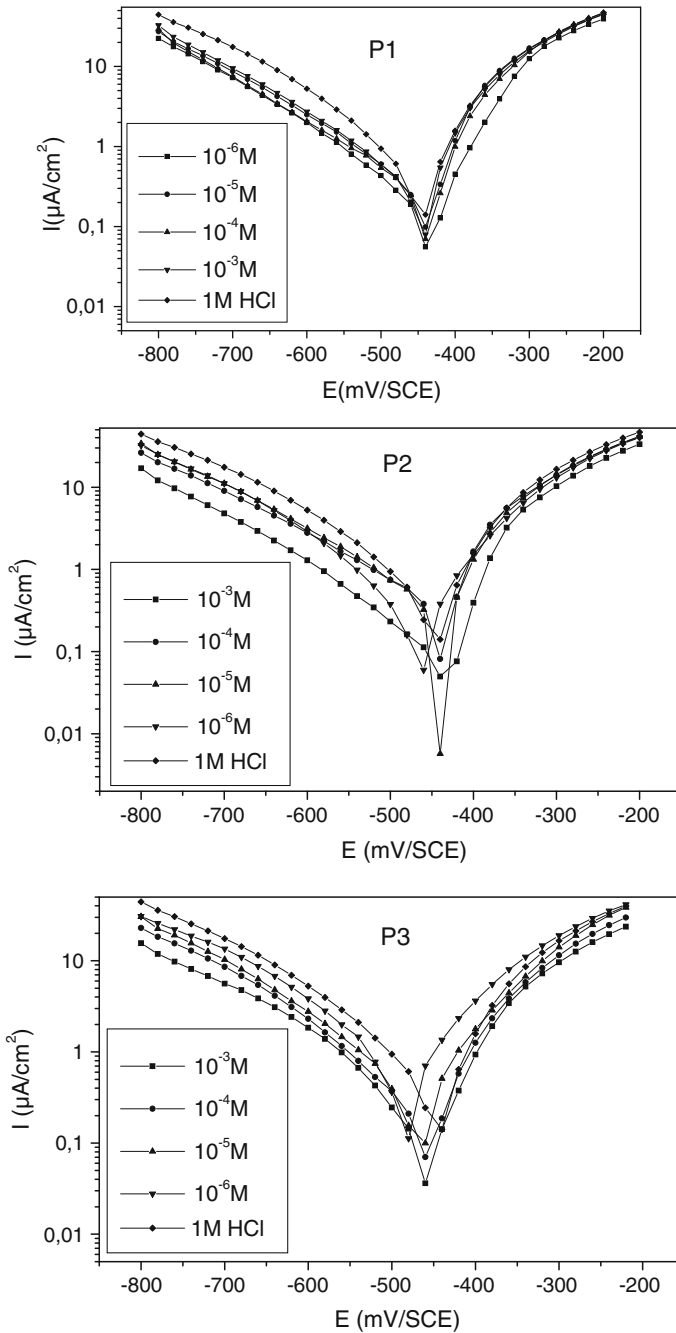


Fig. 2 Polarisation curves for carbon steel in 1 M HCl containing different concentrations of diamine compounds studied at 35 °C

Table 2 Potentiodynamic polarization parameters for corrosion of carbon steel in 1 M HCl with various concentrations of inhibitor at 35 °C

Inhibitor	C (M)	E_{corr} (mV)	b_c (mV/dec)	I_{corr} ($\mu\text{A}/\text{cm}^2$)	E (%)
P1	Blank	-474	177	1,239.6	-
	10^{-6}	-473	176	485.3	60.8
	10^{-5}	-485	178	456.2	63.2
	10^{-4}	-465	180	416.8	66.3
	10^{-3}	-449	172	239.9	80.6
P2	Blank	-474	177	1,239.6	-
	10^{-6}	-479	151	650	47.5
	10^{-5}	-473	183	618	50.1
	10^{-4}	-462	194	520	58.0
	10^{-3}	-456	163	146.3	88.2
P3	Blank	-474	177	1,239.6	-
	10^{-6}	-505	170	890.7	28.1
	10^{-5}	-487	169	531	57.2
	10^{-4}	-474	169	347	71.9
	10^{-3}	-471	181	284	77.0

temperature. To determine the action energy of the corrosion process, gravimetric measurements were taken at various temperatures (313–353 K) in the absence (W_0) and presence of inhibitor **P1** (W_1), inhibitor **P2** (W_2), and inhibitor **P3** at 10^{-3} M after 1 h of immersion. The corresponding results are given in Table 3.

It is clear that the increase of the corrosion rate is more pronounced with the rise of temperature for the blank solution. In the presence of the tested molecules, W_{corr} is reduced even at high temperature. E (%) passed from 97.3 to 60.3% when the temperature rises from 313 to 353 K at 10^{-3} M of **P2**. We note that the efficiency of the inhibitors tested depends on the temperature and decreases with the rise of temperature from 313 to 353 K.

The logarithm of the corrosion rate of steel W_{corr} can be represented as a straight-line function of $1,000/T$ (Arrhenius equation; Fig. 3), where T is the temperature in Kelvin.

The activation energy could be determined from Arrhenius plots for the steel corrosion rate, presented in Fig. 3, by the following relationship:

$$w_{\text{corr}}^0 = K^0 \exp\left(-\frac{E_a^0}{RT}\right) \text{ and } w_{\text{corr}} = K \exp\left(-\frac{E_a}{RT}\right) \quad (2)$$

where E_a and E_a^0 are the activation energies for the corrosion in the presence and absence of inhibitors, respectively.

From these results, we note that the addition of inhibitors in acid solution apparently affects the value of the activation energy of the corrosion reaction. This phenomenon is often interpreted with chemical adsorption.

Table 3 Effect of temperature on the corrosion rate of steel in 1 M HCl solution (W_0) without and with **P1**, **P2**, and **P3** at 10^{-3} M and the corresponding corrosion inhibition efficiency

Inhibitor	Temperature (K)	Concentration (M)	W (mg cm $^{-2}$ h $^{-1}$)	E (%)	θ
P1	313	Blank	2.6	–	–
		5×10^{-5}	0.3	88.46	0.884
		10^{-4}	0.29	88.84	0.888
		5×10^{-4}	0.24	90.76	0.907
		10^{-3}	0.2	92.30	0.923
	323	Blank	4.8	–	–
		5×10^{-5}	0.76	84.16	0.841
		10^{-4}	0.7	85.41	0.854
		5×10^{-4}	0.6	87.50	0.875
		10^{-3}	0.4	91.66	0.916
	333	Blank	8.8	–	–
		5×10^{-5}	2.2	75.00	0.750
		10^{-4}	1.74	80.22	0.802
		5×10^{-4}	1.5	82.95	0.829
		10^{-3}	1.07	87.84	0.878
	343	Blank	13.2	–	–
		5×10^{-5}	4.2	68.18	0.681
		10^{-4}	3.61	72.65	0.726
		5×10^{-4}	2.42	81.66	0.816
		10^{-3}	1.7	87.12	0.871
353	Blank	26.5	–	–	
	5×10^{-5}	9.8	63.01	0.630	
	10^{-4}	9.4	64.52	0.645	
	5×10^{-4}	6.31	76.18	0.761	
	10^{-3}	5.9	77.73	0.777	
P2	313	Blank	2.6	–	–
		5×10^{-5}	0.36	86.15	0.861
		10^{-4}	0.32	87.69	0.876
		5×10^{-4}	0.17	93.46	0.934
		10^{-3}	0.07	97.30	0.973
	323	Blank	4.8	–	–
		5×10^{-5}	0.7	85.41	0.854
		10^{-4}	0.63	86.87	0.868
		5×10^{-4}	0.32	92.33	0.923
		10^{-3}	0.26	94.58	0.945
	333	Blank	8.8	–	–
		5×10^{-5}	2.3	73.86	0.738
		10^{-4}	1.52	82.72	0.827
		5×10^{-4}	0.85	90.34	0.903
		10^{-3}	0.74	91.59	0.915

Table 3 continued

Inhibitor	Temperature (K)	Concentration (M)	W (mg cm ⁻² h ⁻¹)	E (%)	θ
P3	343	Blank	13.2	–	–
		5×10^{-5}	4.7	64.39	0.643
		10^{-4}	3.15	76.13	0.761
		5×10^{-4}	2.16	83.63	0.836
		10^{-3}	1.96	85.15	0.851
	353	Blank	26.5	–	–
		5×10^{-5}	10.5	60.37	0.603
		10^{-4}	8.24	68.90	0.689
		5×10^{-4}	6.4	75.84	0.758
		10^{-3}	5.5	79.24	0.792
	313	Blank	2.6	–	–
		10^{-4}	0.3	88.46	0.884
		5×10^{-4}	0.24	90.76	0.907
		10^{-3}	0.19	92.69	0.926
		323	Blank	4.8	–
	10^{-4}		0.56	88.33	0.883
	5×10^{-4}		0.5	89.58	0.895
	10^{-3}		0.36	92.50	0.925
	333		Blank	8.8	–
		10^{-4}	1.3	85.22	0.852
5×10^{-4}		0.96	89.09	0.890	
10^{-3}		0.8	90.9	0.909	
343		Blank	13.2	–	–
	10^{-4}	3.1	76.51	0.765	
	5×10^{-4}	2.32	82.42	0.824	
	10^{-3}	1.5	88.63	0.886	
	353	Blank	26.5	–	–
10^{-4}		7.9	70.18	0.701	
5×10^{-4}		6	77.35	0.773	
10^{-3}		3.2	87.92	0.879	

Adsorption

Basic information on the interaction between the inhibitor and the carbon steel can be provided by the adsorption isotherm. Two main types of interaction can describe the adsorption of the organic compounds: physical adsorption and chemisorption. These are influenced by the chemical structure of the inhibitor, the type of the electrolyte and the charge and nature of the metal. The surface coverage θ of the metal surface by the adsorbed inhibitor was calculated [27] assuming no change in the mechanism of the cathodic reaction using the equation:

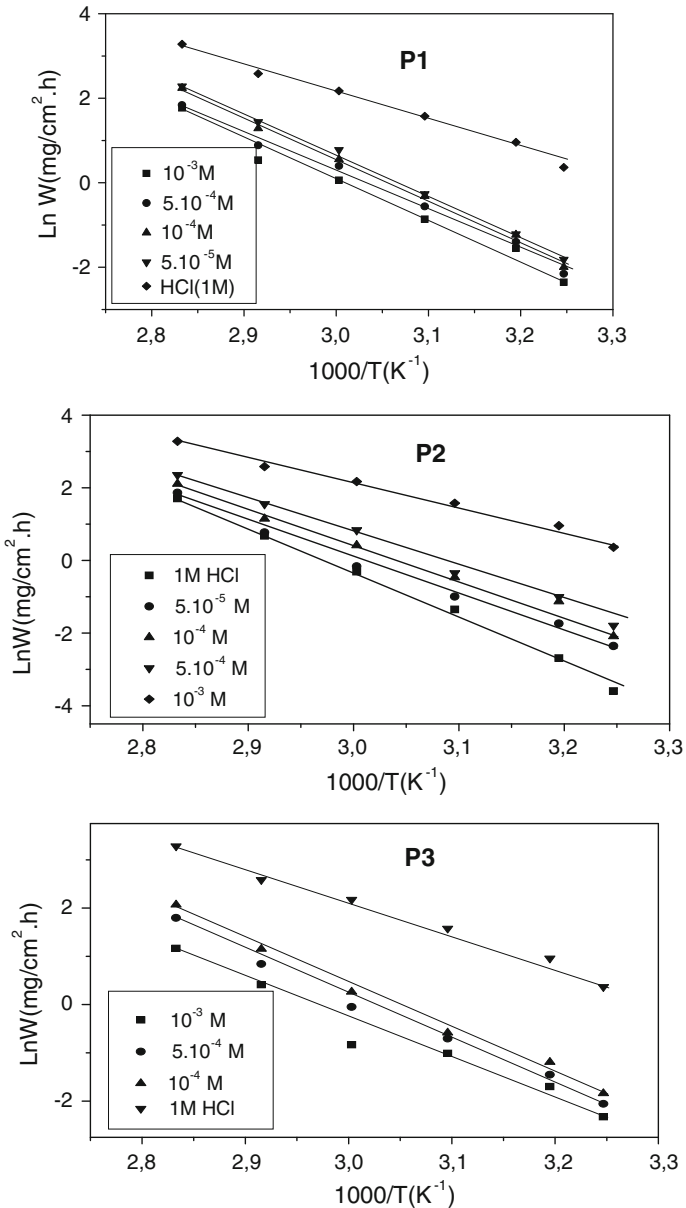


Fig. 3 Arrhenius plots for steel in 1 M HCl in the absence and presence of **P1**, **P2**, and **P3**

$$\theta = \frac{W_0 - W}{W_0} \quad (3)$$

where W_0 and W are the corrosion rates in the absence and presence of the inhibitors, respectively.

The θ values for different inhibitor concentrations at 35–80 °C were tested by fitting to various isotherms. By far the best fit was obtained with the Langmuir adsorption isotherm. According to this isotherm, θ is related to concentration inhibitor C via;

$$\frac{C}{\theta} = \frac{1}{K} + C \quad (4)$$

$$K = \frac{1}{55.5} \exp\left(-\frac{\Delta G_{\text{ads}}^0}{RT}\right) \quad (5)$$

where K is the adsorptive equilibrium constant and ΔG_{ads}^0 is the free energy of adsorption.

It was found that Fig. 4 (plot of θ/C vs. C) gives straight lines with slope equal or nearly equal to 1 for 40, 50, 60, 70, and 80 °C. This result indicates that the adsorption of compound under consideration on the steel/acidic solution interface at all temperatures follows the Langmuir adsorption isotherm.

Thermodynamic parameters are important to study the inhibitive mechanism. The values of ΔG_{ads}^0 at different temperatures were estimated from the values of K and Eq. 5. The negative values of ΔG_{ads}^0 show that the adsorption of the organic compounds studied is a spontaneous process [28] under the experimental conditions described. It is well known that values of ΔG_{ads}^0 of the order of 20 kJ mol⁻¹ or lower indicate a physisorption, while those of the order of 40 kJ mol⁻¹ or higher involve charge sharing or a transfer from the inhibitor molecules to the metal surface to form a co-ordinate type of bond [29, 30]. On the other hand, Metikoš-Huković et al. [31] describe the interaction between thiourea and iron ($\Delta G_{\text{ads}}^0 = -39$ kJ mol⁻¹) as chemisorption. The same conclusion was given by Wang et al. [32] concerning the interaction between mercapto-triazole and MS ($\Delta G_{\text{ads}}^0 = -32$ kJ mol⁻¹). Moreover, Bayoumi and Ghanem [33] consider that the adsorption of naphthalene disulphonic acid on the MS was principally by chemisorption ($\Delta G_{\text{ads}}^0 = -28.47$ kJ mol⁻¹). Thus, the ΔG_{ads}^0 value obtained here shows that, in the presence of 1 M HCl, chemisorption of inhibitors on the MS may occur.

Considering the values of enthalpy and entropy of the inhibition process have no distinct changes in the temperature range studied, the thermodynamic parameters ΔH_{ads}^0 and ΔS_{ads}^0 for the adsorption of **P1**, **P2**, and **P3** on carbon steel can be calculated from the following equation:

$$\Delta G_{\text{ads}}^0 = \Delta H_{\text{ads}}^0 - T\Delta S_{\text{ads}}^0 \quad (6)$$

where ΔH_{ads}^0 and ΔS_{ads}^0 are the variation of enthalpy and entropy of the adsorption process, respectively. The values of ΔG_{ads}^0 were plotted against T . This plot is shown in Fig. 5. It should be noted that the entropy change of adsorption $-\Delta S_{\text{ads}}^0$ is the slope of the straight line $\Delta G_{\text{ads}}^0 - T$ according to Eq. 6. The intercept of the straight line is used to calculate the heat of adsorption ΔH_{ads}^0 . The calculated values are depicted in Table 4. The negative sign of ΔH_{ads}^0 indicates that the adsorption of inhibitor molecules is an exothermic process. ΔS_{ads}^0 in the presence of inhibitor is

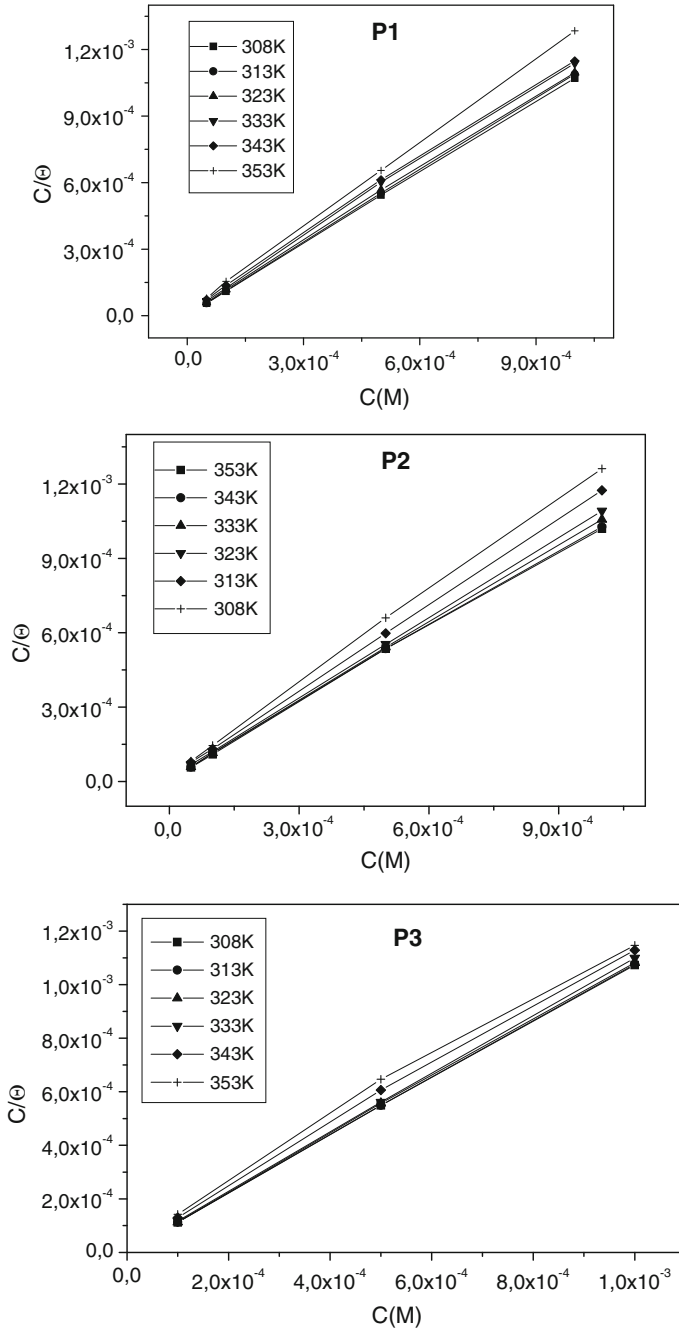


Fig. 4 Langmuir adsorption plots for carbon steel in 1 M HCl containing different concentrations of inhibitor at different temperatures

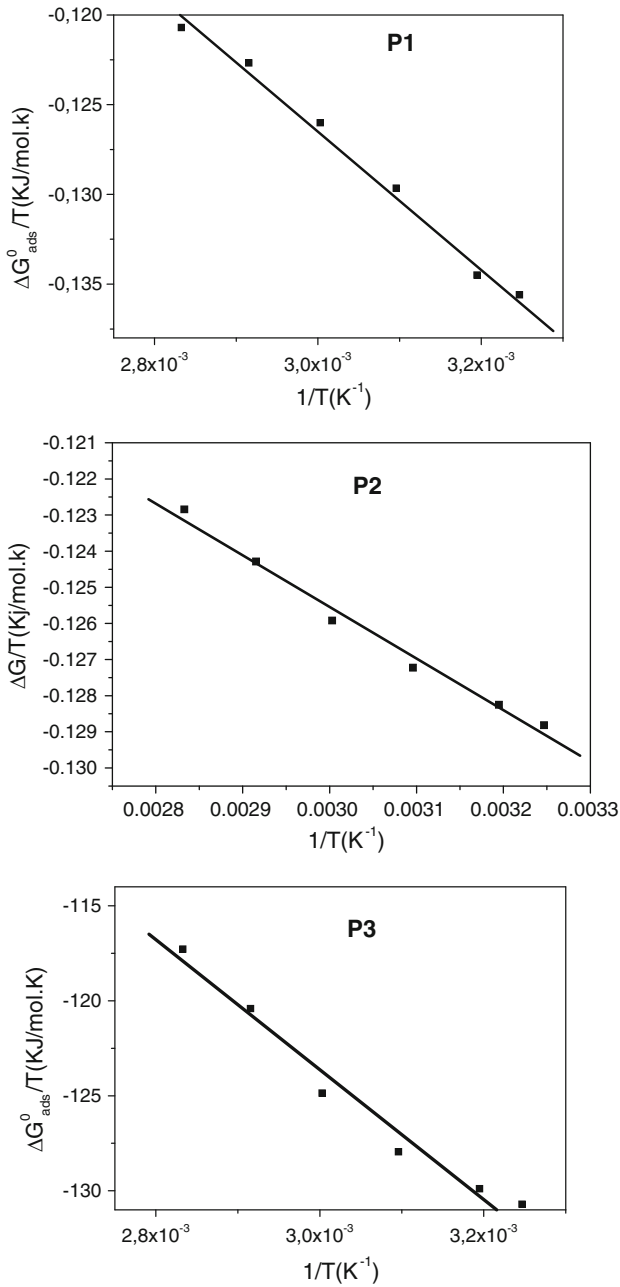


Fig. 5 The relationship between ΔG^0_{ads} and T

Table 4 The thermodynamic parameters for some diamine compounds studied at the carbon steel surface in 1 M HCl solution

Inhibitor	Temperature (K)	K^a	B^b	ΔG_{ads}^0 (kJ mol ⁻¹)	ΔH_{ads}^0 (kJ mol ⁻¹)	ΔS_{ads}^0 (J mol ⁻¹ K ⁻¹)
P1	308	215,616.68	1.07	-41.76	-38.56	10.4
	313	232,885.80	1.08	-42.64	-38.56	13
	323	102,139.20	1.09	-41.78	-38.56	9.9
	333	61,616.95	1.13	-41.68	-38.56	9.3
	343	38,578.46	1.13	-41.59	-38.56	8.8
	353	44,736.32	1.26	-43.24	-38.56	13.2
P2	308	88,958.47	1.01	-39.49	-14.29	8.2×10^{-2}
	313	76,091.34	1.02	-39.72	-14.29	8.12×10^{-2}
	323	103,711.63	1.05	-41.83	-14.29	8.52×10^{-2}
	333	73,297.66	1.08	-42.16	-14.29	8.37×10^{-2}
	343	55,388.46	1.16	-42.63	-14.29	8.26×10^{-2}
	353	41,141.42	1.24	-43.00	-14.29	8.13×10^{-2}
P3	308	107,220.43	1.06	-39.97	-34.19	18.77
	313	105,260.83	1.07	-40.57	-34.19	20.72
	323	93,820.95	1.07	-41.56	-34.19	23.54
	333	90,883.47	1.09	-42.76	-34.19	26.53
	343	32,119.94	1.1	-41.07	-34.19	20.07
	353	18,974.64	1.1	-40.72	-34.19	18.51

^a Equilibrium constant of adsorption

^b Slope value of Langmuir adsorption isotherm

large and positive, meaning that an increase in disordering takes place in going from reactants to the metal adsorbed species reaction complex [34].

Moreover, since adsorption enthalpy is small and negative and adsorption entropy is large and positive, it can be assumed that the driving force for the adsorption of adsorbate is the increase in entropy during the process of adsorption rather than the decrease in enthalpy.

On the other hand, ΔH_{ads}^0 can also be calculated according to the Van't Hoff equation:

$$\ln K = \frac{-\Delta H_{\text{ads}}^0}{RT} + \text{constant} \quad (7)$$

Figure 6 shows the plot of $\ln K$ versus $1/T$ which gives straight lines with slopes of $\Delta H_{\text{ads}}^0/R$ and intercept of ΔH_{ads}^0 . The calculated ΔH_{ads}^0 using the Van't Hoff equation confirms the exothermic behavior of the adsorption of some diamine compounds on the steel surface. Values of ΔH_{ads}^0 obtained by both methods are in good agreement. Moreover, the assumed ΔS_{ads}^0 value is very close to that given in Table 4.

In the present study, chemisorption is evident from the apparent activation energy of the corrosion, that is lower in the presence of some diamine compounds than in

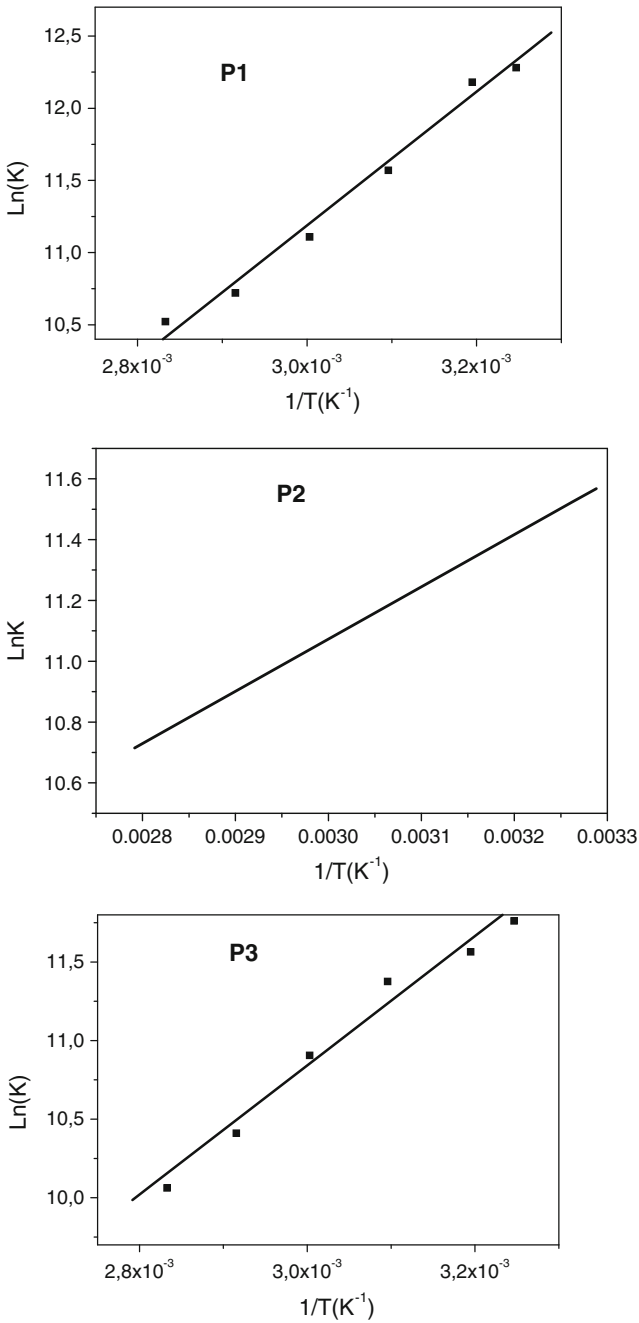


Fig. 6 The relationship between ln (K) and 1/T

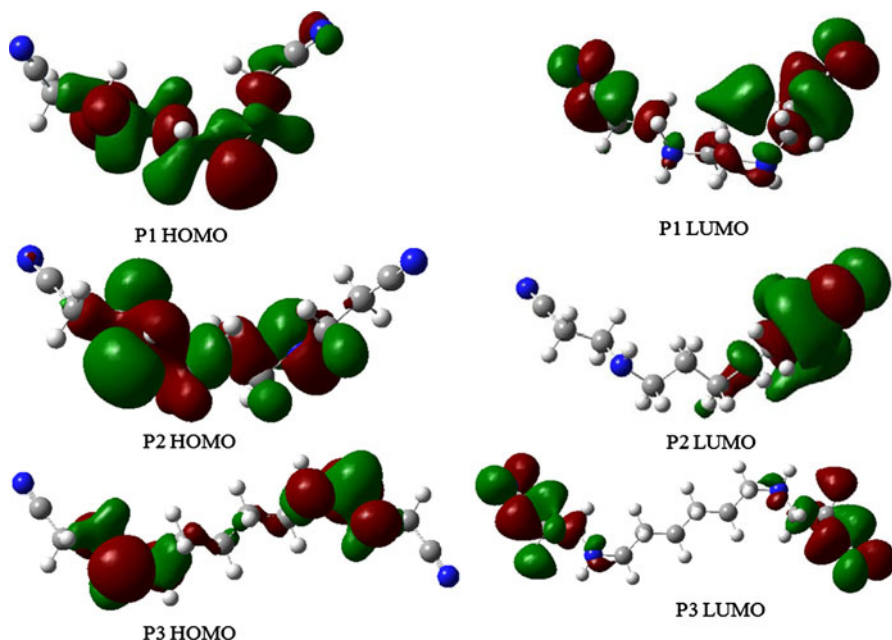


Fig. 7 Calculated HOMO and LUMO molecular orbitals of the studied molecules **P1**, **P2**, and **P3** in their neutral form

Table 5 The calculated quantum chemical parameters of the studied molecules

	P1	P2	P3
E_{HOMO} (eV)	-6.1703	-6.4333	-5.8476
E_{LUMO} (eV)	0.7343	0.8038	-0.7401
ΔE (eV)	6.9046	7.2371	5.1075
μ (debye)	6.1967	4.4668	6.0001
E_{W} (%)	93.3	98	93.1
$I = -E_{\text{HOMO}}$ (eV)	6.1703	6.4333	5.8476
$A = -E_{\text{LUMO}}$ (eV)	-0.7343	-0.8038	0.7401
$\chi = \frac{I+A}{2}$ (eV)	2.718	2.814	3.2938
$\eta = \frac{I-A}{2}$ (eV)	3.452	3.618	2.553
$\sigma = \frac{1}{\eta}$	0.289	0.276	0.391
TE (u.a.)	-532.22998	-571.54711	-685.67387

their absence, the inhibition efficiency, which is temperature independent, and the large negative values of ΔG_{ads}^0 . Therefore, organic compounds may adsorb on a metal surface in the form of a neutral molecule via the chemisorption mechanism [35] involving the sharing of electrons between the nitrogen atoms and iron.

Table 6 The calculated quantum chemical parameters of the studied molecules in their protonated form

	P1	P2	P3
E_{HOMO} (eV)	-10.283	-9.707	-8.386
E_{LUMO} (eV)	-4.504	-4.396	-4.317
ΔE (eV)	5.779	5.311	4.069
μ (debye)	8.8937	8.7181	20.7674
E_W (%)	93.3	98	93.1
$I = -E_{\text{HOMO}}$ (eV)	10.283	9.707	8.386
$A = -E_{\text{LUMO}}$ (eV)	4.504	4.396	4.317
$\chi = \frac{I+A}{2}$ (eV)	7.166	7.0515	6.351
$\eta = \frac{I-A}{2}$ (eV)	2.889	2.655	2.034
$\sigma = \frac{1}{\eta}$	0.346	0.376	0.491
TE (u.a.)	-532.58827	-571.9066	-689.8502

The covalent bond with the metal is most probably formed between the unpaired electrons of the N-atom.

Theoretical results

Quantum chemical calculations were performed to investigate the effect of structural electronic parameters on the inhibition efficiency of inhibitors. Previous studies confirmed the fact that, in aqueous acidic solution, these types of compounds get protonated and exist either as neutral molecules or in the form of cations. The studied compounds may adsorb on the metal surface in the form of neutral molecules or in the form of protonated molecules. Geometric and electronic structures of the inhibitors were calculated by the complete geometrical optimization in their neutral and protonated form. The obtained molecular structures and HOMO and LUMO orbitals of the neutral inhibitor molecules by DFT/B3LYP/6-31G*(d) obtained from the DFT calculations are given in Fig. 7.

Quantum chemical parameters are obtained from the calculations which are responsible for the inhibition efficiency of inhibitors such as the energies of HOMO (E_{HOMO}), energy of LUMO (E_{LUMO}), energy gap (ΔE), dipole moment (μ), electronegativity (χ), electron affinity (A), global hardness (η), softness (σ), ionization potential (I), and the TE are shown in Table 5.

The energy of HOMO is often associated with the electron-donating ability of a molecule. Therefore, the energy of LUMO indicates the ability of the molecule to accept electrons [36, 37]. So, when we compared the studied compounds **P1**, **P2**, and **P3**, the calculations show that the compound **P2**, which has the highest inhibition efficiency, has the highest LUMO level and lowest HOMO. On the other hand, when we examine the obtained values of gap energies, the results obtained show that the compound **P2** has a high value of ΔE gap. This parameter provides a measure for the stability of the formed complex on the metal surface. Even in the literature the correlation between ΔE gap and inhibition efficiency is often cited.

Our theoretical results indicate that no significant relationship was detected between ΔE gap and inhibition efficiency. The most widely used quantity to describe the polarity is the dipole moment of the molecule [38]. Dipole moment is the measure of polarity of a polar covalent bond. It is defined as the product of the charge on the atoms and the distance between the two bonded atoms. The total dipole moment, however, reflects only the global polarity of a molecule. For a complete molecule, the total molecular dipole moment may be approximated as the vector sum of individual bond dipole moments. The calculations show that the compound **P2** has the lowest value of dipole moment. Indeed, the inhibition efficiency decreases with increasing dipole moment. The theoretical study has shown that quantum chemical parameters such as hardness (η) and softness (σ) were well correlated with the inhibition efficiency when we compared the studied compounds, the calculations showing that the compound **P2** has the highest value of hardness (η) and a low value of softness (σ). Indeed, the inhibition efficiency increases with increasing hardness. Other quantum chemical parameters such as electronegativity (χ), electron affinity (A), ionization potential (I), and the TE were also calculated. Our theoretical results indicate that no significant relationship was detected between these parameters and inhibition efficiency.

On the other hand, in an acidic medium, these molecules could be easily protonated; the calculated quantum chemical parameters of the protonated compounds are shown in Table 6. The results show that protonation produces a remarkable change of all the calculated quantum chemical parameters. So, there is a considerable effect on the reactivity which should be considered. Comparing quantum chemical results for neutral and protonated inhibitors, E_{HOMO} as well as E_{LUMO} values decreased in the case of the protonated inhibitors which reflects the decreasing of reactivity due to the protonation, but there is no correlation with the experimental result. Also, it could be noticed that the protonated molecules exhibit high dipole moment in the following order **P3** > **P1** > **P2**. The protonated compound **P2** has the lowest value of dipole moment. Indeed, the inhibition efficiency decreases with increasing dipole moment. So, we expect that the dipole moment will play an important role in the adsorption of protonated inhibitors on the metal surface.

Conclusion

The following conclusions are drawn:

- The diamine derivatives inhibit the corrosion of steel in 1 M HCl solution. The inhibition efficiency increases with the inhibitor concentration.
- Inhibitors act essentially as mixed type inhibitors.
- The adsorption of inhibitors on the steel surface from 1 M HCl solution follows the Langmuir adsorption isotherm. The adsorption process is a spontaneous and exothermic process.
- The inhibition efficiency of organic compounds decreases in the temperature range 313–353 K.

- The results obtained from weight loss and potentiodynamic polarisation are all in good agreement.
- From the obtained results and by using the DFT calculations, the inhibition efficiency of the studied compounds **P1**, **P2**, and **P3** was investigated leading to the following conclusions:
 - Using the B3LYP/6-31 G(d) method, the inhibition efficiency of the studied compound may be correlated to their molecular structure.
 - The calculated dipole moments, the softness, and hardness show reasonably good correlation with the efficiency of corrosion inhibition and no significant relationship was found with the other parameters.
 - All studied inhibitors have a considerable tendency for protonation and this process produces a remarkable change of all the calculated quantum chemical parameters. Also, it could be concluded from the calculations that the protonated molecules exhibit high dipole moment in the following order **P3 > P1 > P2**.
 - Comparing quantum chemical results for neutral and protonated inhibitors, E_{HOMO} as well as E_{LUMO} values decreased in the case of the protonated inhibitors which reflects the decreasing of reactivity due to the protonation, but there is no correlation with the experimental result.

References

1. S.A. Ali, M.T. Saeed, S.V. Rahman, *Corros. Sci.* **45**, 253 (2003)
2. K.C. Pillai, R. Narayan, *Corros. Sci.* **2**, 3 (1983)
3. J.O.M. Bockris, J. McBreen, L. Nanis, *J. Electrochem. Soc.* **112**, 1025 (1965)
4. F. Bentiss, M. Traisnel, H. Vezin, H.F. Hildebrand, M. Lagrenée, *Corros. Sci.* **46**, 2781 (2004)
5. M. Lagrenée, B. Mernari, M. Bouanis, M. Traisnel, F. Bentiss, *Corros. Sci.* **44**, 573 (2002)
6. G. Trabanelli, *Corrosion* **47**, 410 (1991)
7. J.M. Sykes, *Br. Corros. J.* **25**, 175 (1990)
8. G. Lewis, *Corros. Sci.* **22**, 579 (1982)
9. S. Rengamani, T. Vasudenvan, S. Vka Iyer, *Indian J. Technol.* **31**, 519 (1993)
10. G. Schmitt, *Br. Corros. J.* **19**, 165 (1984)
11. J.O.M. Bockris, B. Yang, *J. Electrochem. Soc.* **138**, 2237 (1991)
12. K. Chandrasekara Pillai, R. Narayan, *Corros. Sci.* **23**, 151 (1983)
13. F.B. Growcock, V.R. Lopp, *Corros. Sci.* **28**, 397 (1988)
14. M. Bartos, N. Hackerman, *J. Electrochem. Soc.* **139**, 3428 (1992)
15. F. Zucchi, G. Trabanelli, G. Brunoro, *Corros. Sci.* **33**, 1135 (1992)
16. B.M. Mistry, N.S. Patel, N.J. Patel, S. Jauhari, *Res. Chem. Intermed.* **37**, 659 (2011)
17. J. Cruz, T. Pandiyan, E. García-Ochoa, *J. Electroanal. Chem.* **583**, 8 (2005)
18. J. Cruz, R. Martínez, E. Genesca, E. García-Ochoa, *J. Electroanal. Chem.* **566**, 111 (2004)
19. C. Ogretir, G. Bereket, Quantum chemical studies of some pyridine derivatives as corrosion inhibitors. *J. Mol. Struct. (Theochem.)* **488**, 223 (1999)
20. M.J. Frisch, G.W. Trucks, H.B. Schlegel, G.E. Scuseria, M.A. Robb, J.R. Cheeseman, J.A. Montgomery Jr., T. Vreven, K.N. Kudin, J.C. Burant, J.M. Millam, S.S. Iyengar, J. Tomasi, V. Barone, B. Mennucci, M. Cossi, G. Scalmani, N. Rega, G.A. Petersson, H. Nakatsuji, M. Hada, M. Ehara, K. Toyota, R. Fukuda, J. Hasegawa, M. Ishida, T. Nakajima, Y. Honda, O. Kitao, H. Nakai, M. Klene, X. Li, J.E. Knox, H.P. Hratchian, J.B. Cross, C. Adamo, J. Jaramillo, G.A. Voth, P. Salvador, J.J. Dannenberg, V.G. Zakrzewski, S. Dapprich, A.D. Daniels, M.C. Strain, O. Farkas, D.K. Malick, A.D. Rabuck, K. Raghavachari, J.B. Foresman, J.V. Ortiz, Q. Cui, A.G. Baboul, S. Clifford, J. Cioslowski, B.B. Stefanov, G. Liu, A. Liashenko, P. Piskorz, I. Komaromi, R.L. Martin, D.J. Fox, T. Keith, M.A.

- Al-Laham, C.Y. Peng, A. Nanayakkara, M. Challacombe, P.M.W. Gill, B. Johnson, W. Chen, M.W. Wong, C. Gonzalez, J.A. Pople, *Gaussian 03, Revision C.02* (Gaussian Inc., Pittsburgh, 2003)
21. S.G. Zhang, Z. Lei, M.Z. Xia, F.Y. Wang, QSAR study on N containing corrosion inhibitors: quantum chemical approach assisted by topological index. *J. Mol. Struct. (Theochem.)* **732**, 175 (2005)
 22. M. Lashgari, M.R. Arshadi, G.A. Parsafar, A simple and fast method for comparison of corrosion inhibition powers between pairs of pyridine derivative molecules. *Corrosion* **61**, 778 (2005)
 23. V.S. Sastri, J.R. Perumareddi, *Corrosion* **53**, 671 (1996)
 24. R.G. Pearson, *Inorg. Chem.* **27**, 734 (1988)
 25. F. Touhami, A. Aouniti, Y. Abed, B. Hammouti, S. Kertit, A. Ramdani, K. Elkacemi, *Corros. Sci.* **42**, 929 (2000)
 26. B.G. Ateya, B.M. Abo El-Khair, I.A. Abdel Hamid, *Corros. Sci.* **16**, 163 (1976)
 27. T. Tsuru, S. Haruyama, B. Gijutsu, *J. Jpn. Soc. Corros. Eng.* **27**, 573 (1978)
 28. A.E. Fouda, H.A. Mostafa, H.M. Abu-Elnader, *Monatshefte. für. Chem.* **104**, 501 (1989)
 29. F.M. Donahue, K. Nobe, *J. Electrochem. Soc.* **112**, 886 (1965)
 30. E. Kamis, F. Belluci, R.M. Latanision, E.S.H. El-Ashry, *Corrosion* **47**, 677 (1991)
 31. M. Metikoš-Huković, R. Babić, Z. Grubać, *J. Appl. Electrochem.* **26**, 443 (1996)
 32. H.L. Wang, H.B. Fan, J.S. Zheng, *Mater. Chem. Phys.* **77**, 655 (2002)
 33. F.M. Bayoumi, W.A. Ghanem, *Mater. Lett.* **59**, 3806 (2005)
 34. F. Xu, J. Duan, S. Zhang, B. Hou, *Mater. Lett.* **62**, 4072 (2008)
 35. M.P. Soriaga, *Chem. Rev.* **90**, 771 (1990)
 36. L. Larabi, Y. Harek, O. Benali, S. Ghalem, *Prog. Org. Coat.* **54**, 256 (2005)
 37. I. Lukovits, I. Bako, A. Shaban, E. Kalman, *Electrochim. Acta* **43**, 131 (1998)
 38. O. Kikuchi, Systematic QSAR procedures with quantum chemical descriptors. *Quant. Struct.-Act. Relatsh.* **6**, 179 (1987)